Published in final edited form as:
J Recept Signal Transduct Res. 2010 October ; 30(5): 304–312. doi:10.3109/10799893.2010.509728.

Theme and variations on kinetics of GPCR activation/deactivation

Jean-Pierre Vilardaga[1,2]

[1] Laboratory for GPCR Biology, Department of Pharmacology and Chemical Biology, University of Pittsburgh, School of Medicine, Pittsburgh, PA 15261, USA

[2] Endocrine Unit, Department of Medicine, Massachusetts General Hospital and Harvard Medical School, MA 02114, USA

Abstract

G protein-coupled receptors (GPCRs) initiate intracellular signaling pathways in response to physiologically and medically important extracellular ligands such as peptide and large glycoprotein hormones, neurotransmitters, sensory stimuli (odorant and taste molecules, light), calcium, L-amino acids, and are the target of many clinical drugs. The conversion of these extracellular stimuli into intracellular signals involves sequential and reversible reactions that initially take place at the plasma membrane. These reactions are mediated not only by dynamic interactions between ligands, receptors and heterotrimeric G proteins, but also by conformational changes associated with the activation/deactivation process of each protein. This review discusses the kinetic characteristics and rate-limiting reactions engaged in signal propagation that are involved in systems as diverse as neurotransmitter and hormonal signaling, and that have been recorded in live cells by Förster resonance energy transfer (FRET) approaches.

Keywords

GPCR; kinetics; FRET

Introduction

Specialized seven α-helical transmembrane proteins known as G protein-coupled receptors (GPCRs) constitute the largest family of cell surface proteins in the human genome and serve as molecular switches to transmit extracellular stimuli into cell signaling cascades (1–5). The initial steps in GPCR signaling take place in the plasma membrane and involve the binding of a ligand (L) that rapidly shifts the inactive receptor (R) to an active state (R*). In the following steps the activated receptor couples to and activates heterotrimeric G proteins (G) through the release of a bound guanosine diphosphate (GDP) and the capture of guanosine triphosphate (GTP) on the G protein α-subunit (Gα) (6–9). The GDP/GTP exchange proceeds through a series of intra and intermolecular events in the heterotrimer Gαβγ that results in active Gα-GTP and Gβγ subunits (10–14). Both Gα and Gβγ proteins can then signal independently to their effector proteins, either enzymes (adenylate cyclase isoforms, phospholipase C) or channels (voltage-gated calcium-, and G protein-activated inwardly rectifying K^+ channels) (15–17). The timing of a GPCR signaling cascade is

Address for Correspondence: J.-P. Vilardaga, Laboratory for GPCR Biology, Department of Pharmacology and Chemical Biology, University of Pittsburgh, School of Medicine, Pittsburgh, E1357, 200 Lothrop street, Pittsburgh, PA 15261, USA. jpv@pitt.edu.

Declaration of interest
The author reports no conflicts of interest.

controlled by a dynamic interplay between a sequence of reactions involving ligand/receptor interaction, receptor/G protein interaction, as well as conformational changes associated with the activation/deactivation cycles of receptors and G proteins (18–22).

A series of spectroscopic and fluorescent techniques applied to purified and reconstituted receptors revealed that the molecular nature of receptor activation is associated with a conformational rearrangement of the receptor's transmembrane helices relative to one another, particularly helices 3 and 6 (23–26). These studies are limited, however, by the difficulty of recording fast kinetics of ligand-induced conformational changes that would be compatible with the biological response to receptor activation occurring within seconds in live cells (27,28). This limitation has been bypassed by the use of Förster resonance energy transfer (FRET) approaches, which allow the recording kinetics of receptor activation in real-time in live cells (see below). This review discusses kinetics and rate-limiting reactions that proceed along diverse GPCR signaling systems, and which have been recorded by live cell microscopy with genetically encoded FRET-based biosensors (Figure 1A, 1D, and 1G).

Kinetic diversity in GPCR signaling systems

Ligand binding

The temporal events of both ligand binding to, and unbinding from a receptor expressed in a live cell can be measured by FRET between a receptor *N*-terminally tagged with green fluorescent (GFP) protein and a ligand, usually a peptide, tagged with a red fluorophore such as tetramethylrhodamine (TMR) (29). The principle of this experiment is that resonance energy transfer occurs when part of the energy from the GFP (the donor fluorophore) in the *N*-terminal extracellular domain of a receptor is transferred to TMR (the acceptor fluorophore) attached to the ligand (Figure 1A). In the absence of binding, GFP and TMR are not in close proximity, the energy is not transferred and only green light emitted by GFP is detected. When GFP and TMR are brought into close proximity by means of the specific binding between the ligand and the receptor, energy is transferred from GFP to TMR resulting in the emission of red light from TMR and a simultaneous decrease in emission of green light from GFP. The time course of this decrease in GFP fluorescence is thus a means to measure real-time kinetics of ligand/receptor association. This approach has determined the kinetics of ligand binding for two distinct GPCR systems: the neurokinin NK2 receptor and the parathyroid hormone type 1 receptor (PTHR; Figure 2A) (29–32). For both receptors, agonist association is the result of a two-step process in which the kinetics of the first binding step reflect a simple bimolecular interaction (L + R) between the ligand (L) and the receptor (R) that is strictly dependent on ligand concentrations. In the case of PTH, for example, the initial time constant is ≈ 150 ms at 10 μM of PTH-related peptide PTHrP(1–36) (Figure 1C, and 2A). The second binding step involves slower kinetics with time constants that follow a hyperbolic dependence on ligand concentration, suggesting a more complex mechanism involving ligand/receptor interactions as well as conformational changes of the ligand and the receptor (Figure 1C). The two distinct rate constants recorded for the NK2 receptor are thought to reflect either the induction or the stabilization of two different receptor conformations. The fastest is associated with Ca^{2+} signaling only and the slowest is linked to cAMP signaling. A distinct scenario has been demonstrated for the PTHR, where a rapid first phase mirrored ligand binding to the receptor *N*-domain (*N*-terminal extracellular domain), and the second phase reflected association to the J-domain (comprising the seven transmembrane helices and connecting extracellular loops) exhibiting much slower kinetics. The second binding phase is temporally coupled to the isomerization of the complex ligand-receptor with an active conformation, which in turn triggers G protein activation (29,30,33,34). The time constants of this slower binding step at different concentrations of agonist match those observed for receptor activation, as measured with a

FRET-based biosensor for receptor activation (see below), and are thus rate limiting for activation of the PTHR (Figure 2A).

The kinetics of agonist dissociation have also been measured and analyzed for the PTHR (Figure 2B) (30,35). The dissociation of PTHrP(1–36) proceeds through a two-step mechanism of ligand release involving a fast and slow components. One of these components reflects a rapid dissociation process (τ = 1.3 sec), which corresponds to a small fraction (~15%) of ligand-bound receptor; the other component corresponds to a slower dissociation process (τ = 28 sec). The ability a dominant negative form of Gαs (DN-G_S), which forms a stable but inactive signaling complex with Gαs-coupled receptors, to eliminate most (~80%) of the slow phase of the ligand dissociation process suggests that the slow dissociation component is dependent on the release of G proteins from the receptor (Figure 2C) (30).

Receptor activation/deactivation

The kinetics of receptor activation and deactivation can be measured by recording intramolecular FRET changes from receptor biosensors (20,36–39). These receptors are made with the cyan fluorescent protein (CFP, the donor) inserted in the third intracellular loop of a receptor and the yellow fluorescent protein (YFP, the acceptor) fused to the C-terminus of the same receptor or *vice et versa* (Figure 1D) (33). Alternatively, the tetracysteine motif CCPGCC can be used as an acceptor in place of YFP. This sequence binds specifically the membrane permeable dye molecule FlAsH (Fluorescein Arsenical Hairpin binder, the acceptor) and has the advantage of being a much smaller molecule than YFP (40). Diverse functional receptor biosensors, referred to as $GPCR^{FlAsH/CFP}$ or $GPCR^{YFP/CFP}$, have been generated that report with high temporal resolution ligand-induced receptor's switches by recording changes in intramolecular FRET (33,40–47). The CFP/FlAsH FRET pair can report GPCR activation in living cells at least as well as FRET from CFP/YFP and sometimes with larger amplitude of the FRET signal (40). The conformational rearrangements that take place as the receptor switches from an inactive to an active state upon agonist binding are transmitted to the FRET pair and modify the relative distance and/or dipole–dipole orientation between the fluorescent partners, which results in a rapid loss of FRET (Figure 1E). This FRET change can be monitored as the change in the ratio of emission intensities of yellow and cyan fluorescences, F_{YFP}/F_{CFP}. This usually follows a monoexponential time course (Figure 1E). The time constant (τ) of receptor activation follows a hyperbolic dependence on ligand concentrations and reaches a minimal value at saturating concentrations of agonist (33). This behavior usually represents a two-step process where ligand-receptor collisions are rate limiting, at first, followed by a slower step in which the receptor undergoes a conformational switch. The fastest speed observed for receptor activation in response to small agonist molecules ranges between time constants of ≈ 40 and 100 ms in the case of α_{2A}- and β_1-adrenergic receptors, adenosine α_{2A}-receptor, and muscarinic M_1- and M_2-receptors (33,40,41,43,46). The speed of receptor activation, however, is considerably slower ($\tau \approx 1$ sec) for the PTHR even in response to a full agonist (30,33; Table 1). Differences in the activation time course of these distinct receptors may not only depend on intrinsic properties of receptors themselves, but also on the type of ligand and its mode of binding to the receptor. Additional interactions of receptors with other receptors, or single transmembrane protein members of the receptor activity-modifying protein family, or adapter proteins such as the Na^+/H^+ exchanger regulatory factor adaptor protein, may stabilize distinct receptor conformations that modulate kinetics of GPCR activation.

Kinetics of receptor deactivation, measured by recording the increase in FRET after ligand washout (Figure 1E), are also variable for each type of receptor. Deactivation of α_{2A}AR and M_2R after ligand removal proceed with a time constant of $\tau \approx 1$–2 sec (43,48), whereas

PTHR deactivation is much slower with a $\tau \approx 58$ sec after PTHrP(1–36) washout (30). These kinetic differences may depend not only on differences in ligand structure (small molecules vs. peptides) and binding affinity, but also on the intrinsic capacity of activated receptors to switch back to their inactive state. For example, bound PTHrP(1–36) labeled with TMR ($PTHrP^{TMR}$) dissociates from the PTHR *N*-terminally tagged with GFP (^{GFP}N-PTHR) with a half-time $t_{1/2}$ of ≈ 19 sec, whereas the PTHR biosensor ($PTHR^{CFP/YFP}$) deactivates with $t_{1/2} = 40$ sec after $PTHrP^{TMR}$ washout (30). Given that $PTHrP^{TMR}$ bound to ^{GFP}N-PTHR exhibits binding isotherms and signaling properties similar to unlabeled PTHrP bound to $PTHR^{CFP/YFP}$ (30), one deduction would be that ligand dissociation is completed before receptor deactivation. The active state of the PTHR, thus, persists even after PTHrP(1–36) has dissociated. As a result of slow receptor deactivation relative to the rate of ligand dissociation, the receptor remains in its active state for an extended time, which presumably permits multiple cycles of G protein activation.

Kinetics of receptor activation and ligand efficacy

Different ligands acting at a receptor can produce variable responses corresponding to their varying intrinsic efficacies, and which are independent of the maximal occupancy of receptors (49,50). Agonists can either generate a maximal (full agonists) or submaximal (partial agonists) receptor-mediated response, or reduce (inverse agonists) basal levels of receptor signaling. Studies in live cells have reported that ligands of different efficacies produced changes in FRET signals from cells expressing $GPCR^{CFP/YFP}$ or $GPCR^{FlAsH/CFP}$ that correspond to their expected pharmacological properties: full and partial agonists decrease FRET with diverse magnitudes, whereas inverse agonists increase FRET (33,41,44,51). Ligand efficacies can therefore be measured not only as conformational changes of a different character, but also of different kinetics. For example, FRET changes reporting conformational rearrangements of the α_{2A}AR are fast for full agonists ($\tau \approx 50$ ms), slower for partial agonists ($t < 1$ sec), and even slower ($\tau \approx 1$ sec) for inverse agonists (41,51). These varying kinetics depend on neither structural nor binding affinity differences between ligands, but instead correlate remarkably well with the functional efficacy of each tested ligand, as measured by the level and kinetics of G protein activity, also recorded by FRET assays (see below) (Figure 3). These differences have been interpreted as evidence that ligands with different efficacies can switch a receptor into distinct conformational states, which in turn determine the kinetics and magnitude of G protein signaling. These FRET-based data thus support a model in which differences in agonist efficacy at the level of G protein activation and signaling originate from distinct conformations of the receptor (52–56).

Fast receptor deactivation by allosteric modulation

Interactions of allosteric compounds at allosteric receptor sites (i.e. separate from the binding site for the native ligand) or conformational changes from one receptor to another can modulate receptor activity by processes involving rapid conformational changes (57–62). A recent work shows that gallamine and dimethyl-W84, two negative allosteric ligands at the M_2 muscarinic receptor, block agonist-induced receptor signals as measured by a FRET-based muscarinic M_2 receptor sensor, $M_2R^{FlAsH/CFP}$ (43). These allosteric ligands do not trigger receptor signaling or changes in FRET by themselves, but instead reverse the FRET response to receptor-agonist binding (i.e., increase of FRET rather than decrease it). This allosteric effect occurs rapidly, with a time constant of $\tau \approx 80$–200 ms at saturating concentrations of gallamine or dimethyl-W84.

A cross-conformational change that propagates from one receptor to another can also act as a rapid allosteric modulator of receptor activity. This has been experimentally demonstrated through FRET microscopy for the α_{2A}-adrenergic receptor and the μ-opioid receptor, which

form receptor heterodimers in neurons and cultured cells (α_{2A}AR/μOR) (42). These receptors, which can act either singly or as heteromers, stimulate common signaling pathways through the inhibitory G_i protein in response to their respective endogenous agonists (63). In this case, morphine binding to the μ-opioid receptor alters the activation of the α_{2A}-adrenergic receptor through a trans-conformational change transmitted from the μOR to the α_{2A}AR. The kinetics of this change is rapid ($t_{1/2}$ < 400 ms) and faster than that of G protein activation (Figure 4). This fast trans-conformational switch between receptors decreases both activation of G_i signaling and stimulation of MAP kinase phosphorylation (36). Thus, conformational cross-talk between receptors prevents over stimulation of signaling pathways to two different ligands acting on a receptor heteromer by rapidly adjusting the extent of G protein activation.

Receptor-G protein interaction

The kinetics of receptor and G protein interaction can be measured by recording intermolecular FRET between a receptor C-terminally tagged with a GFP variant (e.g. CFP) and a Gγ or Gβ subunit *N*-terminally tagged with CFP (Figure 1G) (48,64). Upon agonist exposure a fast increase in FRET most likely reflects the interaction between the ligand-bound receptor and the G protein (Figure 1H). The speed of this interaction typically is dependent on the relative expression levels of receptors and G proteins, in accord with a diffusion-controlled process and contradictory a precoupling model (Figure 1I); (30,64). For the PTHR, the maximum time constant obtained at a high level of G_S is 0.96 sec at a saturating concentration of PTH, and is identical to that obtained for the corresponding PTHR activation switch (30). However, in the context of a low level of G protein or PTHR, the time constant of the PTHR/G_S interaction can take a few seconds whereas the rate of receptor activation remains unchanged. The kinetic rate of the PTHR/G_S interaction is not therefore determined by the time course of receptor activation, but rather by a diffusion-controlled collision process. A similar scenario has been reported for the α_{2A}AR/Gi and adenosine A_2R/G_S systems (48,64).

G protein activation/deactivation

Kinetics of G protein activation, the following step, are measured by the time course of FRET changes between CFP inserted into the Gα subunit, and YFP fused to the *N*-terminus of either Gβ or Gγ (11,12,65). Conformational and/or dissociational events associated with G protein activation usually yielded a decrease, or in some case an increase, in FRET. For example, an increase in FRET was found for activation of G_i proteins containing $G\alpha_{i1,2,3}$, whereas a decrease in FRET was observed for G_o protein activation (12,66). These FRET data suggest that G protein activation in live cells may proceed through conformational rearrangement between α and βγ subunits rather than complete subunits dissociation (67). Kinetics of FRET changes associated with G protein activation reach maximal values with time constants of $\tau \approx 1$–2 sec at a saturating concentration of agonists such as PTHrP(1–36), norepinephrine, or oxotremodine acting at the PTHR, α_{2A}AR, and M_1R, respectively (12,30,46). Fastest kinetics ($\tau \approx 0.5$ sec) have been reported for G_S activation mediated by β_1AR and α_{2A}R in response to norepinephrine and adenosine, their respective agonists (44,48). Following ligand washout, G proteins deactivate with much slower kinetics than that observed for receptor deactivation (Table 1). For example, the time course of G protein deactivation is ≈ twofold slower than that of PTHR deactivation, and is even slower than deactivation of α_{2A}AR, β_1AR, α_{2A}R, and M_1R (Table 1). The slowness of G protein deactivation relative to the faster deactivation of receptors is not only compatible with the slow intrinsic GTPase activity of Gα-subunits, but also with additional steps involving Gα and Gβγ trafficking inside the cell (68–71). Overexpression of the G protein biosensor also may limit the action of GTPase-activating proteins (GAPs) known to accelerate the Gα-mediated GTP hydrolysis (72).

Conclusions

The temporal resolution of key biochemical reactions involved in GPCR signaling can be experimentally measured in real-time and in live cells by using quantitative FRET-based approaches. These methods, recently reviewed (20,36), allow the kinetics and rate-limiting reactions for each step along the GPCR signaling cascade to be determined. This opens new possibilities to dissect mechanisms involved in the initiation and termination of signal cascades, and to determine the molecular origin of signal differences mediated by the binding of different ligands to the same receptor, as well as the rate-limiting step that determines the duration of a signaling response.

Acknowledgments

This work was supported by the National Institutes of Health (NIH) grant DK087688. I thank Tim Feinstein for critical comments.

References

1. Jacoby E, Bouhelal R, Gerspacher M, Seuwen K. The 7 TM G-protein-coupled receptor target family. ChemMedChem. 2006; 1:761–782. [PubMed: 16902930]
2. Pierce KL, Premont RT, Lefkowitz RJ. Seven-transmembrane receptors. Nat Rev Mol Cell Biol. 2002; 3:639–650. [PubMed: 12209124]
3. Kristiansen K. Molecular mechanisms of ligand binding, signaling, and regulation within the superfamily of G-protein-coupled receptors: molecular modeling and mutagenesis approaches to receptor structure and function. Pharmacol Ther. 2004; 103:21–80. [PubMed: 15251227]
4. Rasmussen SG, Choi HJ, Rosenbaum DM, Kobilka TS, Thian FS, Edwards PC, Burghammer M, Ratnala VR, Sanishvili R, Fischetti RF, Schertler GF, Weis WI, Kobilka BK. Crystal structure of the human beta2 adrenergic G-protein-coupled receptor. Nature. 2007; 450:383–387. [PubMed: 17952055]
5. Rosenbaum DM, Rasmussen SG, Kobilka BK. The structure and function of G-protein-coupled receptors. Nature. 2009; 459:356–363. [PubMed: 19458711]
6. Bourne HR, Sanders DA, McCormick F. The GTPase superfamily: conserved structure and molecular mechanism. Nature. 1991; 349:117–127. [PubMed: 1898771]
7. Linderman JJ. Modeling of G-protein-coupled receptor signaling pathways. J Biol Chem. 2009; 284:5427–5431. [PubMed: 18940812]
8. Kaziro Y, Itoh H, Kozasa T, Nakafuku M, Satoh T. Structure and function of signal-transducing GTP-binding proteins. Annu Rev Biochem. 1991; 60:349–400. [PubMed: 1909108]
9. Selinger Z. Discovery of G protein signaling. Annu Rev Biochem. 2008; 77:1–13. [PubMed: 17506637]
10. Lambert NA. Uncoupling diffusion and binding in FRAP experiments. Nat Methods. 2009; 6:183. author reply 183–183; author reply 184. [PubMed: 19247290]
11. Janetopoulos C, Jin T, Devreotes P. Receptor-mediated activation of heterotrimeric G-proteins in living cells. Science. 2001; 291:2408–2411. [PubMed: 11264536]
12. Bünemann M, Frank M, Lohse MJ. Gi protein activation in intact cells involves subunit rearrangement rather than dissociation. Proc Natl Acad Sci USA. 2003; 100:16077–16082. [PubMed: 14673086]
13. Galés C, Van Durm JJ, Schaak S, Pontier S, Percherancier Y, Audet M, Paris H, Bouvier M. Probing the activation-promoted structural rearrangements in preassembled receptor-G protein complexes. Nat Struct Mol Biol. 2006; 13:778–786. [PubMed: 16906158]
14. Yi TM, Kitano H, Simon MI. A quantitative characterization of the yeast heterotrimeric G protein cycle. Proc Natl Acad Sci USA. 2003; 100:10764–10769. [PubMed: 12960402]
15. Wettschureck N, Offermanns S. Mammalian G proteins and their cell type specific functions. Physiol Rev. 2005; 85:1159–1204. [PubMed: 16183910]

16. Smrcka AV. G protein betagamma subunits: central mediators of G protein-coupled receptor signaling. Cell Mol Life Sci. 2008; 65:2191–2214. [PubMed: 18488142]
17. Dupré DJ, Robitaille M, Rebois RV, Hébert TE. The role of Gbetagamma subunits in the organization, assembly, and function of GPCR signaling complexes. Annu Rev Pharmacol Toxicol. 2009; 49:31–56. [PubMed: 18834311]
18. Lamb TD. Gain and kinetics of activation in the G-protein cascade of phototransduction. Proc Natl Acad Sci USA. 1996; 93:566–570. [PubMed: 8570596]
19. Pugh EN Jr, Lamb TD. Amplification and kinetics of the activation steps in phototransduction. Biochim Biophys Acta. 1993; 1141:111–149. [PubMed: 8382952]
20. Vilardaga JP, Bünemann M, Feinstein TN, Lambert N, Nikolaev VO, Engelhardt S, Lohse MJ, Hoffmann C. GPCR and G proteins: drug efficacy and activation in live cells. Mol Endocrinol. 2009; 23:590–599. [PubMed: 19196832]
21. Ross EM. Coordinating speed and amplitude in G-protein signaling. Curr Biol. 2008; 18:R777–R783. [PubMed: 18786383]
22. Turcotte M, Tang W, Ross EM. Coordinate regulation of G protein signaling via dynamic interactions of receptor and GAP. PLoS Comput Biol. 2008; 4:e1000148. [PubMed: 18716678]
23. Farrens DL, Altenbach C, Yang K, Hubbell WL, Khorana HG. Requirement of rigid-body motion of transmembrane helices for light activation of rhodopsin. Science. 1996; 274:768–770. [PubMed: 8864113]
24. Altenbach C, Yang K, Farrens DL, Farahbakhsh ZT, Khorana HG, Hubbell WL. Structural features and light-dependent changes in the cytoplasmic interhelical E-F loop region of rhodopsin: a site-directed spin-labeling study. Biochemistry. 1996; 35:12470–12478. [PubMed: 8823182]
25. Farahbakhsh ZT, Hideg K, Hubbell WL. Photoactivated conformational changes in rhodopsin: a time-resolved spin label study. Science. 1993; 262:1416–1419. [PubMed: 8248781]
26. Yao X, Parnot C, Deupi X, Ratnala VR, Swaminath G, Farrens D, Kobilka B. Coupling ligand structure to specific conformational switches in the beta2-adrenoceptor. Nat Chem Biol. 2006; 2:417–422. [PubMed: 16799554]
27. Jensen AD, Guarnieri F, Rasmussen SG, Asmar F, Ballesteros JA, Gether U. Agonist-induced conformational changes at the cytoplasmic side of transmembrane segment 6 in the beta 2 adrenergic receptor mapped by site-selective fluorescent labeling. J Biol Chem. 2001; 276:9279–9290. [PubMed: 11118431]
28. Gether U, Lin S, Kobilka BK. Fluorescent labeling of purified beta 2 adrenergic receptor. Evidence for ligand-specific conformational changes. J Biol Chem. 1995; 270:28268–28275. [PubMed: 7499324]
29. Castro M, Nikolaev VO, Palm D, Lohse MJ, Vilardaga JP. Turn-on switch in parathyroid hormone receptor by a two-step parathyroid hormone binding mechanism. Proc Natl Acad Sci USA. 2005; 102:16084–16089. [PubMed: 16236727]
30. Ferrandon S, Feinstein TN, Castro M, Wang B, Bouley R, Potts JT, Gardella TJ, Vilardaga JP. Sustained cyclic AMP production by parathyroid hormone receptor endocytosis. Nat Chem Biol. 2009; 5:734–742. [PubMed: 19701185]
31. Palanche T, Ilien B, Zoffmann S, Reck MP, Bucher B, Edelstein SJ, Galzi JL. The neurokinin A receptor activates calcium and cAMP responses through distinct conformational states. J Biol Chem. 2001; 276:34853–34861. [PubMed: 11459843]
32. Lecat S, Bucher B, Mely Y, Galzi JL. Mutations in the extracellular amino-terminal domain of the NK2 neurokinin receptor abolish cAMP signaling but preserve intracellular calcium responses. J Biol Chem. 2002; 277:42034–42048. [PubMed: 12185075]
33. Vilardaga JP, Bünemann M, Krasel C, Castro M, Lohse MJ. Measurement of the millisecond activation switch of G protein-coupled receptors in living cells. Nat Biotechnol. 2003; 21:807–812. [PubMed: 12808462]
34. Dean T, Vilardaga JP, Potts JT Jr, Gardella TJ. Altered selectivity of parathyroid hormone (PTH) and PTH-related protein (PTHrP) for distinct conformations of the PTH/PTHrP receptor. Mol Endocrinol. 2008; 22:156–166. [PubMed: 17872377]
35. Dean T, Linglart A, Mahon MJ, Bastepe M, Jüppner H, Potts JT Jr, Gardella TJ. Mechanisms of ligand binding to the parathyroid hormone (PTH)/PTH-related protein receptor: selectivity of a

modified PTH(1–15) radioligand for GalphaS-coupled receptor conformations. Mol Endocrinol. 2006; 20:931–943. [PubMed: 16339275]

36. Lohse MJ, Bünemann M, Hoffmann C, Vilardaga JP, Nikolaev VO. Monitoring receptor signaling by intramolecular FRET. Curr Opin Pharmacol. 2007; 7:547–553. [PubMed: 17919975]
37. Lohse MJ, Hoffmann C, Nikolaev VO, Vilardaga JP, Bünemann M. Kinetic analysis of G protein-coupled receptor signaling using fluorescence resonance energy transfer in living cells. Adv Protein Chem. 2007; 74:167–188. [PubMed: 17854658]
38. Lohse MJ, Nikolaev VO, Hein P, Hoffmann C, Vilardaga JP, Bünemann M. Optical techniques to analyze real-time activation and signaling of G-protein-coupled receptors. Trends Pharmacol Sci. 2008; 29:159–165. [PubMed: 18262662]
39. Lohse MJ, Vilardaga JP, Bünemann M. Molecular mechanisms of receptor activation: real-time analysis by fluorescence resonance energy transfer. Auton Autacoid Pharmacol. 2003; 23:231–233. [PubMed: 15134067]
40. Hoffmann C, Gaietta G, Bünemann M, Adams SR, Oberdorff-Maass S, Behr B, Vilardaga JP, Tsien RY, Ellisman MH, Lohse MJ. A FlAsH-based FRET approach to determine G protein-coupled receptor activation in living cells. Nat Methods. 2005; 2:171–176. [PubMed: 15782185]
41. Vilardaga JP, Steinmeyer R, Harms GS, Lohse MJ. Molecular basis of inverse agonism in a G protein-coupled receptor. Nat Chem Biol. 2005; 1:25–28. [PubMed: 16407989]
42. Vilardaga JP, Nikolaev VO, Lorenz K, Ferrandon S, Zhuang Z, Lohse MJ. Conformational cross-talk between alpha2A-adrenergic and mu-opioid receptors controls cell signaling. Nat Chem Biol. 2008; 4:126–131. [PubMed: 18193048]
43. Maier-Peuschel M, Frölich N, Dees C, Hommers LG, Hoffmann C, Nikolaev VO, Lohse MJ. A fluorescence resonance energy transfer-based M2 muscarinic receptor sensor reveals rapid kinetics of allosteric modulation. J Biol Chem. 2010; 285:8793–8800. [PubMed: 20083608]
44. Rochais F, Vilardaga JP, Nikolaev VO, Bünemann M, Lohse MJ, Engelhardt S. Real-time optical recording of beta1-adrenergic receptor activation reveals supersensitivity of the Arg389 variant to carvedilol. J Clin Invest. 2007; 117:229–235. [PubMed: 17200720]
45. Nakanishi J, Takarada T, Yunoki S, Kikuchi Y, Maeda M. FRET-based monitoring of conformational change of the beta2 adrenergic receptor in living cells. Biochem Biophys Res Commun. 2006; 343:1191–1196. [PubMed: 16580633]
46. Jensen JB, Lyssand JS, Hague C, Hille B. Fluorescence changes reveal kinetic steps of muscarinic receptor-mediated modulation of phosphoinositides and Kv7.2/7.3 K^+ channels. J Gen Physiol. 2009; 133:347–359. [PubMed: 19332618]
47. Falkenburger BH, Jensen JB, Hille B. Kinetics of M1 muscarinic receptor and G protein signaling to phospholipase C in living cells. J Gen Physiol. 2010; 135:81–97. [PubMed: 20100890]
48. Hein P, Rochais F, Hoffmann C, Dorsch S, Nikolaev VO, Engelhardt S, Berlot CH, Lohse MJ, Bünemann M. Gs activation is time-limiting in initiating receptor-mediated signaling. J Biol Chem. 2006; 281:33345–33351. [PubMed: 16963443]
49. Kenakin T. Drug efficacy at G protein-coupled receptors. Annu Rev Pharmacol Toxicol. 2002; 42:349–379. [PubMed: 11807176]
50. Kenakin T. Efficacy at G-protein-coupled receptors. Nat Rev Drug Discov. 2002; 1:103–110. [PubMed: 12120091]
51. Nikolaev VO, Hoffmann C, Bünemann M, Lohse MJ, Vilardaga JP. Molecular basis of partial agonism at the neurotransmitter alpha2A-adrenergic receptor and Gi-protein heterotrimer. J Biol Chem. 2006; 281:24506–24511. [PubMed: 16787921]
52. Swaminath G, Xiang Y, Lee TW, Steenhuis J, Parnot C, Kobilka BK. Sequential binding of agonists to the beta2 adrenoceptor. Kinetic evidence for intermediate conformational states. J Biol Chem. 2004; 279:686–691. [PubMed: 14559905]
53. Swaminath G, Deupi X, Lee TW, Zhu W, Thian FS, Kobilka TS, Kobilka B. Probing the beta2 adrenoceptor binding site with catechol reveals differences in binding and activation by agonists and partial agonists. J Biol Chem. 2005; 280:22165–22171. [PubMed: 15817484]
54. Seifert R, Gether U, Wenzel-Seifert K, Kobilka BK. Effects of guanine, inosine, and xanthine nucleotides on beta(2)-adrenergic receptor/G(s) interactions: evidence for multiple receptor conformations. Mol Pharmacol. 1999; 56:348–358. [PubMed: 10419554]

55. Seifert R, Wenzel-Seifert K, Gether U, Kobilka BK. Functional differences between full and partial agonists: evidence for ligand-specific receptor conformations. J Pharmacol Exp Ther. 2001; 297:1218–1226. [PubMed: 11356949]
56. Ghanouni P, Gryczynski Z, Steenhuis JJ, Lee TW, Farrens DL, Lakowicz JR, Kobilka BK. Functionally different agonists induce distinct conformations in the G protein coupling domain of the beta 2 adrenergic receptor. J Biol Chem. 2001; 276:24433–24436. [PubMed: 11320077]
57. May LT, Leach K, Sexton PM, Christopoulos A. Allosteric modulation of G protein-coupled receptors. Annu Rev Pharmacol Toxicol. 2007; 47:1–51. [PubMed: 17009927]
58. Christopoulos A, Kenakin T. G protein-coupled receptor allosterism and complexing. Pharmacol Rev. 2002; 54:323–374. [PubMed: 12037145]
59. Kenakin T, Miller LJ. Seven transmembrane receptors as shapeshifting proteins: the impact of allosteric modulation and functional selectivity on new drug discovery. Pharmacol Rev. 2010; 62:265–304. [PubMed: 20392808]
60. Fuxe K, Marcellino D, Rivera A, Diaz-Cabiale Z, Filip M, Gago B, Roberts DC, Langel U, Genedani S, Ferraro L, de la Calle A, Narvaez J, Tanganelli S, Woods A, Agnati LF. Receptor-receptor interactions within receptor mosaics. Impact on neuropsychopharmacology. Brain Res Rev. 2008; 58:415–452. [PubMed: 18222544]
61. Fuxe K, Marcellino D, Guidolin D, Woods AS, Agnati LF. Heterodimers and receptor mosaics of different types of G-protein-coupled receptors. Physiology (Bethesda). 2008; 23:322–332. [PubMed: 19074740]
62. Fuxe K, Canals M, Torvinen M, Marcellino D, Terasmaa A, Genedani S, Leo G, Guidolin D, Diaz-Cabiale Z, Rivera A, Lundstrom L, Langel U, Narvaez J, Tanganelli S, Lluis C, Ferré S, Woods A, Franco R, Agnati LF. Intramembrane receptor-receptor interactions: a novel principle in molecular medicine. J Neural Transm. 2007; 114:49–75. [PubMed: 17066251]
63. Jordan BA, Gomes I, Rios C, Filipovska J, Devi LA. Functional interactions between mu opioid and alpha 2A-adrenergic receptors. Mol Pharmacol. 2003; 64:1317–1324. [PubMed: 14645661]
64. Hein P, Frank M, Hoffmann C, Lohse MJ, Bünemann M. Dynamics of receptor/G protein coupling in living cells. EMBO J. 2005; 24:4106–4114. [PubMed: 16292347]
65. Azpiazu I, Gautam N. A fluorescence resonance energy transfer-based sensor indicates that receptor access to a G protein is unrestricted in a living mammalian cell. J Biol Chem. 2004; 279:27709–27718. [PubMed: 15078878]
66. Frank M, Thümer L, Lohse MJ, Bünemann M. G Protein activation without subunit dissociation depends on a G{alpha}(i)-specific region. J Biol Chem. 2005; 280:24584–24590. [PubMed: 15866880]
67. Lambert NA. Dissociation of heterotrimeric g proteins in cells. Sci Signal. 2008; 1:re5. [PubMed: 18577758]
68. Saini DK, Karunarathne WK, Angaswamy N, Saini D, Cho JH, Kalyanaraman V, Gautam N. Regulation of Golgi structure and secretion by receptor-induced G protein {beta}{gamma} complex translocation. Proc Natl Acad Sci USA. 2010; 107:11417–11422. [PubMed: 20534534]
69. Saini DK, Chisari M, Gautam N. Shuttling and translocation of heterotrimeric G proteins and Ras. Trends Pharmacol Sci. 2009; 30:278–286. [PubMed: 19427041]
70. Chisari M, Saini DK, Kalyanaraman V, Gautam N. Shuttling of G protein subunits between the plasma membrane and intracellular membranes. J Biol Chem. 2007; 282:24092–24098. [PubMed: 17576765]
71. Akgoz M, Kalyanaraman V, Gautam N. G protein betagamma complex translocation from plasma membrane to Golgi complex is influenced by receptor gamma subunit interaction. Cell Signal. 2006; 18:1758–1768. [PubMed: 16517125]
72. Xie GX, Palmer PP. How regulators of G protein signaling achieve selective regulation. J Mol Biol. 2007; 366:349–365. [PubMed: 17173929]

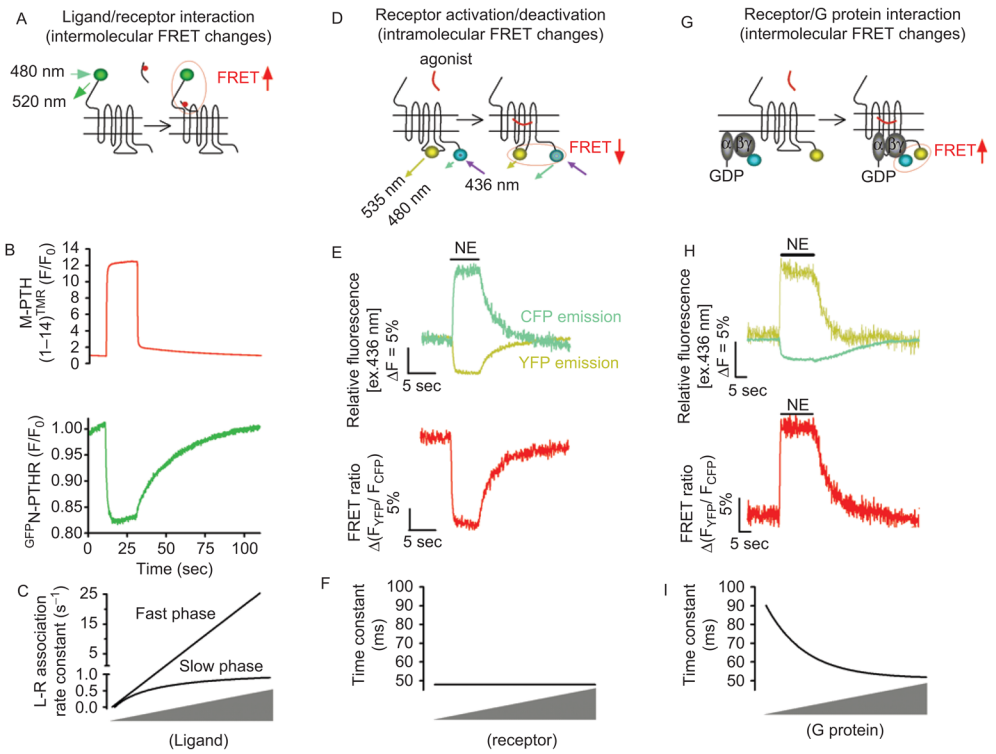

Figure 1.

Application of Förster resonance energy transfer (FRET) for recording initial steps of G protein-coupled receptors (GPCR) signaling in live cells. (A) Kinetics of ligand/receptor interaction are measured under a fluorescence microscope where a single cell was selectively excited at 480 nm [excitation of green fluorescent protein (GFP)], and the changes of the GFP emission fluorescence (515 nm) caused by FRET between a receptor *N*-terminally labeled by GFP (•) and a tetramethylrhodamine (TMR•)-tagged ligand were recorded over time. (B) Example of ligand/receptor interaction measured by FRET between GFP-tagged PTH-receptor (^{GFP}*N*-PTHR) and TMR-labeled PTH analog, M-PTH(1–14)^{TMR}. Shown are the changes of GFP emission by FRET (green signal) in response to rapid superfusion of a PTH analog, M-PTH(1–14)^{TMR} (red signal). (C) Relationship between the rate constants *k* (s^{-1}) and ligand concentration. *k* values for the first component (*k* fast) are directly proportional to the ligand concentration, whereas *k* values for the second step (*k* slow) follow an hyperbolic dependence on ligand concentration and reach a maximal value. (D) For receptor activation/deactivation, experiments are performed under a fluorescence microscope, where light at 436 nm selectively excited a single cell expressing GPCR$^{FlAsH/CFP}$ or GPCR$^{CFP/YFP}$ (for recordings of receptor activation) to induce donor (CFP•) and acceptor (FlAsH or yellow•) emission fluorescences simultaneously recorded over time. FRET is calculated as the ratio of emission intensities F_{YFP}/F_{CFP} after correction for the donor bleed-through into the acceptor emission, the direct acceptor excitation by light at 436 nm, and photobleaching effect. (E) Example of FRET experiments showing direct recordings of norepinephrine (NE)-mediated activation of $\alpha_{2A}AR^{FlAsH/CFP}$ in a single HEK-293 cell. Activation of $\alpha_{2A}AR$ is monitored upon NE application (horizontal bar) by a decrease in the FRET signal (red). (F) Relationship between the time constant of α_{2A}-$AR^{FlAsH/CFP}$ activation after stimulation by NE at a saturating concentration, and receptor concentrations. (G) Receptor/G protein interactions are measured by recording the time course of FRET between a GPCR C-terminally labeled by yellow fluorescent protein and a CFP-labeled Gγ in combination with Gα and Gβ subunits. The principal of these

experiments are similar than those described in Figure 1D. (H) Example of recordings showing the interaction between α_{2A}AR and G_i proteins in response to NE measured as an increase in FRET between YFP-labeled α_{2A}AR and CFP-labeled $G\gamma_2$ in combination with $G\alpha_{i1}$ and $G\beta_1$ proteins. (I) Relationship between the time constant of α_{2A}-AR^{CFP}/$G\alpha_{i1}b_1g_2{}^{YFP}$ interaction after stimulation by NE (100 mM) and G protein concentrations. In this case the kinetics of receptor/G protein interaction depend on expression levels of G_i. (Adapted from ref (20,23,24).) FlAsH, Fluorescein Arsenical Hairpin binder; PTHR, parathyroid hormone type 1 receptor.

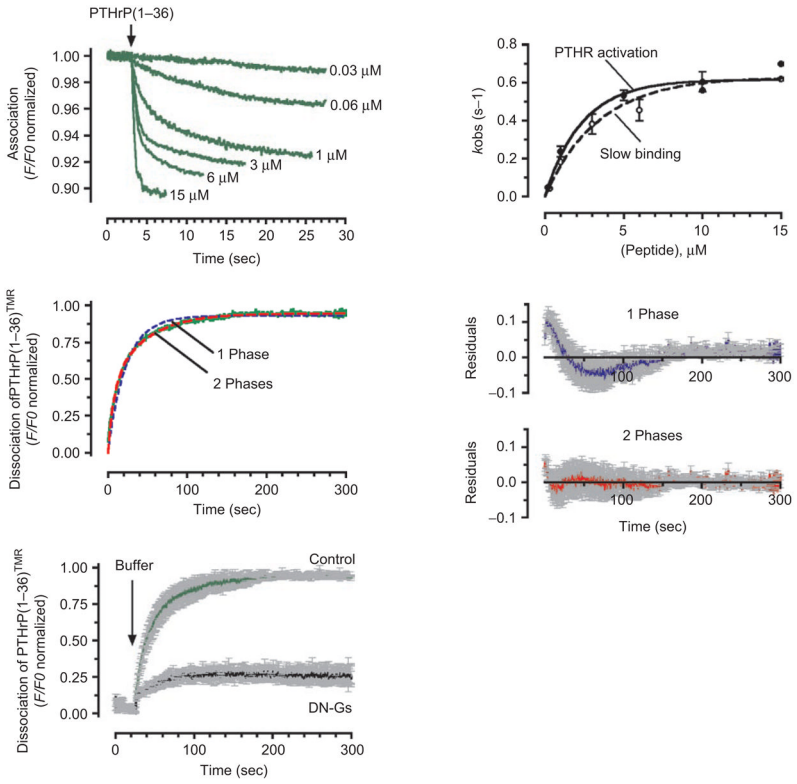

Figure 2.

Kinetics of association and dissociation. (A) Association time courses of PTHrP(1–36)^{TMR} to ^{GFP}N-PTHR are represented by the decrease in the green fluorescent protein (GFP) fluorescence emission. Measurements were recorded in a single HEK-293 cell stably expressing ^{GFP}N-PTHR with various concentrations of PTHrP(1–36)^{TMR} (left panel). Slow rate constants, k_{obs} values (mean ± SEM), obtained from fitting the time course of binding with the sum of two exponential components, followed a hyperbolic dependence on ligand concentrations that coincides those of PTHR activation (right panel). (B) Comparing fits of a one-(blue dashed line) and a two-exponential component (red dashed line) model for the time course of PTHrP(1–36)^{TMR} release (green line). The corresponding of averaged residuals (differences between the experimental data and calculated fitted curves) are plotted in the right panels and indicated that the two-exponential component curve fits the data more accurately. Grey bars represent SD. (C) Averaged dissociation time courses of PTHrP(1–36)^{TMR} from the ^{GFP}N-PTHR are shown in the absence or presence of a dominant negative Gαs (DN-G_S). Förster resonance energy transfer recordings are shown as normalized ratios. Grey bars represent the SEM. The black arrow indicates the time of ligand wash out. (Adapted from refs (24).) PTHR, parathyroid hormone type 1 receptor.

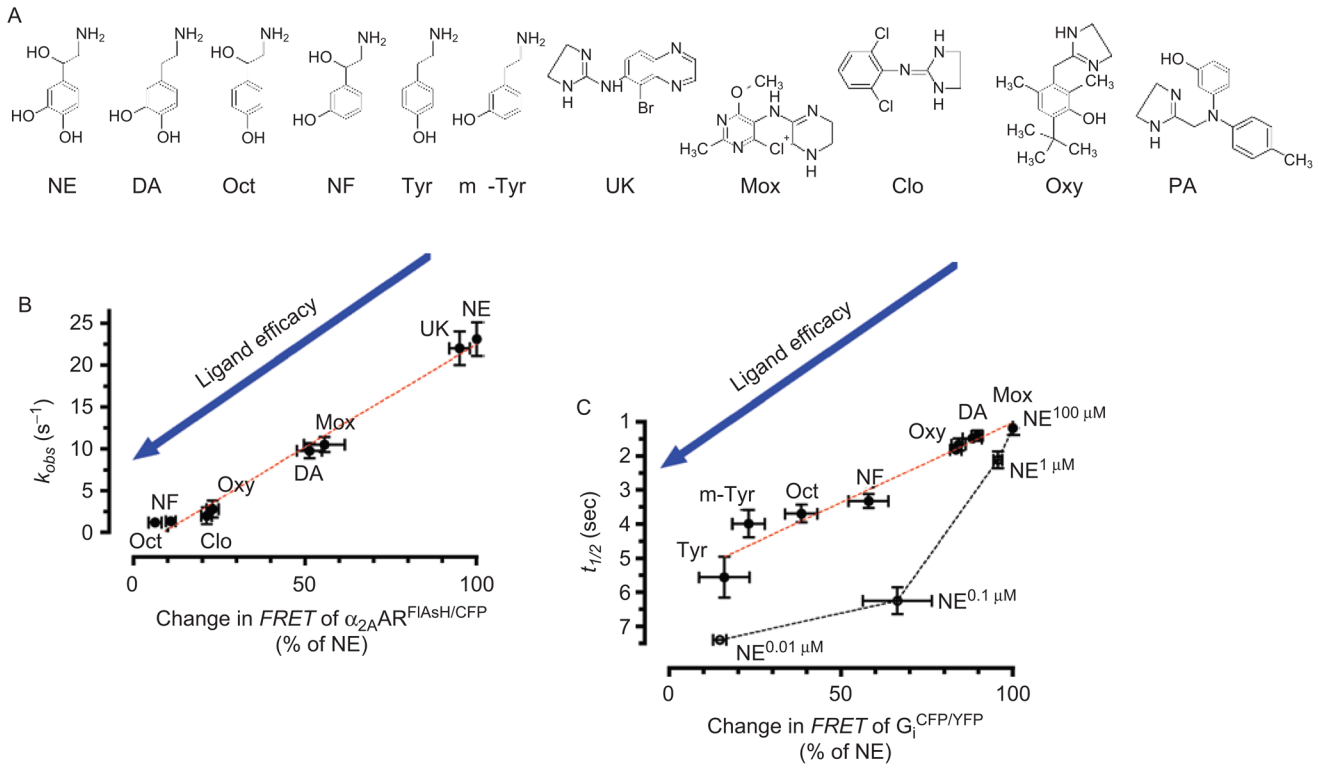

Figure 3.

Linking ligand efficacy and kinetics of receptor activation and G protein activation. (A) Chemical structures of α_{2A}AR agonists: norepinephrine (*NE*), dopamine (*DA*), octopamine (*Oct*), norphenylephrine (*NF*), tyramine (*Tyr*), m-tyramine (*m-Tyr*), UK-14,304 (*UK*) moxonidine (*Mox*), clonidine (*Clo*), oxymetazoline (*Oxy*), and α_{2A}AR-antagonist phentolamine (*PA*). (B) and (C) correlation between kinetics α_{2A}AR activation or Gi activation (measured with the $\alpha_{2A}AR^{CFP/FlAsH}$ and $G\alpha_{i1}{}^{CFP}\beta_1\gamma_2{}^{YFP}$ biosensors, respectively) and agonist efficacy (where efficacy is defined as the ability of an agonist to produce a Förster resonance energy transfer (FRET) response compared with the maximal response achieved by NE) analyzed by linear regression (*red dotted line*), and relation between NE-mediated change in FRET of $G\alpha_{i1}{}^{CFP}\beta_1\gamma_2{}^{YFP}$ and corresponding half-time of Gi activation (*black dotted line*). (Adapted from ref (45).) FlAsH, Fluorescein Arsenical Hairpin binder.

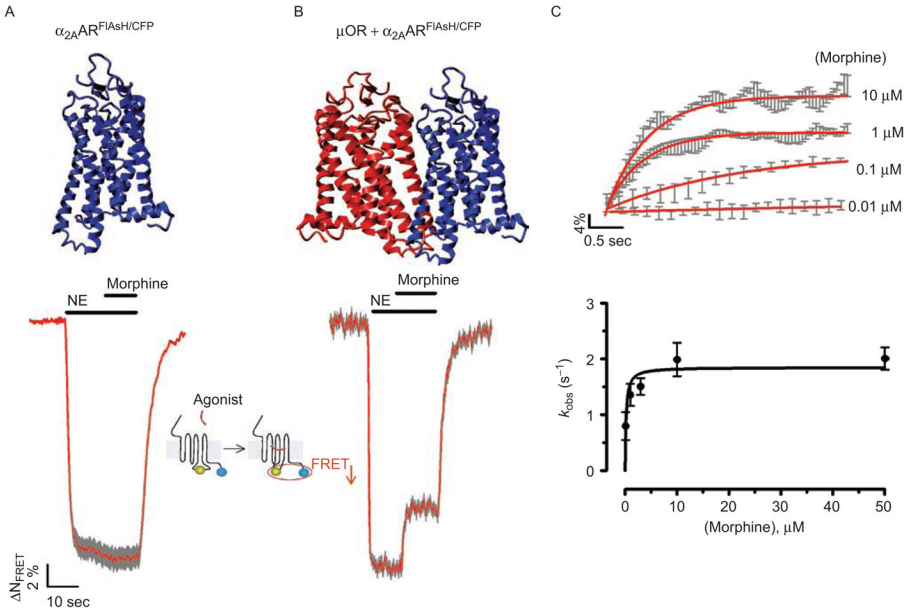

Figure 4.

Trans-conformational switching of the α_{2A}AR by the μOR as an allosteric mechanism underlying direct inhibition of receptor activation. (A) and (B) Time-resolved changes of the Förster resonance energy transfer (FRET) ratio in a single HEK-293 cell expressing the $\alpha_{2A}AR^{FlAsH/CFP}$ (left panels) or co-expressing $\alpha_{2A}AR^{FlAsH/CFP}$ and μOR (A). The red trace represents normalized FRET signals and grey bars represent SD. Horizontal bars indicate the application of norepinephrine (NE) or morphine to the cell. (C) The *top panel* represents the averaged inhibition of NE (50 μM)-mediated $\alpha_{2A}AR^{FlAsH/CFP}$ activation by different concentrations of morphine on cells co-expressing $\alpha_{2A}AR^{FlAsH/CF}$ and μOR (from data similar to those in Figure 4B). The *lower panel* represents the relationship between the apparent rate constant k_{obs} of inhibition of NE (50 μM)-mediated receptor activation and morphine concentrations. k_{obs} values were obtained from fitting the averaged kinetic data from the top panel to a monoexponential equation. (Adapted from ref (36).) FlAsH, Fluorescein Arsenical Hairpin binder.

Table 1

Kinetics of diverse GPCR signaling systems measured by FRET.

	Association or activation(s)					Dissociation or deactivation(s)				
Receptor	**α_{2A}AR**	**β_1AR**	**α_{2A}R**	**M_1R**	**PTHR**	**α_{2A}AR**	**β_1AR**	**α_{2A}R**	**M_1R**	**PTHR**
$L + R \rightleftarrows LR$	nd	nd	nd	nd	$^{\text{Fast}}_{\text{Slow}}$ 0.17 1.54	nd	nd	nd	nd	$^{\text{Fast}}_{\text{Slow}}$ 1.40 28.00
$LR \rightleftarrows LR^*$	0.045	0.060	0.066	< 0.100	1.59	2.00	2.50	4.00	0.20	58.00
$LR^* + G \rightleftarrows LR^*G$	0.045	0.060	0.050	0.200	1.58	≈ 10	8	15	3.70	48.00
$G \rightleftarrows G^*$	≈1.00	0.450	0.450	2.00	2.04	38	15	37	35.00	121

Values represent the time constant (τ).

FRET, Förster resonance energy transfer; GPCR, G protein-coupled receptors; nd, not determined; PTHR, parathyroid hormone type 1 receptor. Ligand (L) and receptor (R) association and dissociation ($L + R \rightleftarrows LR$); receptor activation and deactivation ($LR \rightleftarrows LR^*$); receceptor and G protein (G) interaction ($LR^* + G \rightleftarrows LR^* G$); G activation and deactivation ($G \rightleftarrows G^*$). Reactions were recorded from live cells at a saturating concentration of an agonist: PTHrP(1–36) for PTHR; NE for α_{2A}AR and β_1AR; adenosine for A_{2A}R; oxotremodine-methiodide for M_1R.